Supplementary materials

Construction of Rh doped $SrTiO_3$/g-C_3N_4 p-n heterojunction for enhanced photoelectrochemical performance

Feng Nan,[*a] Songtao Chen,[a] Shun Wang,[*b] Yi Lin,[a] Baolu Fan,[a] Hao Li ,[*c] and Lei Zhou [*a]

[a] Faculty of Mathematics and Physics, Huaiyin Institute of Technology, Huaian, 223003, Jiangsu, China

[b] School of Electronic and Information Engineering, Changshu Institute of Technology, Suzhou, 215000, Jiangsu, China

[c] State Key Laboratory of Radio Frequency Heterogeneous Integration, College of Physics and Optoelectronic Engineering, Key Laboratory of Optoelectronic Devices and Systems of Ministry of Education and Guangdong Province, Shenzhen University, Shenzhen, 518060, Guangdong, China

[*] Corresponding authors:

fengnan@hyit.edu.cn (Feng Nan), swang@cslg.edu.cn (Shun Wang), lihao000000@163.com (Hao Li), leizhou@hyit.edu.cn (Lei Zhou).

1. The morphology, FTIR, and XRD of g-C_3N_4

To further gain more information of g-C_3N_4, the TEM were carried out. Fig. S1(a) and 1(b) display the TEM and HRTEM images of the g-C_3N_4 sample. The measured result displays a typical layered nanosheet structure, and the lattice spacing of 0.325 nm can be ascribed to the hexagonal (002) plane of g-C_3N_4. In addition, Figure S1(c) displays the FTIR curves of g-C_3N_4 sample. For the pure g-C_3N_4, the peaks located at 810 cm^{-1}, 1200-1600 cm^{-1}, and 2900-3500 cm^{-1} can be attributed the breathing vibration of triazine units, C-N/C=N bonds, and N-H bonds, respectively. Figure S1(d) demonstrated the XRD patterns for g-C_3N_4 sample. There are two diffraction peaks located at 13.2° and 27.3° can be observed, attributed to the (100) and (002) crystal planes with an intralayer long-range order and an interlayer stacking structure, respectively.[1] Based on the analysis, the g-C_3N_4 sample has been successfully prepared by the thermal polymerization method.

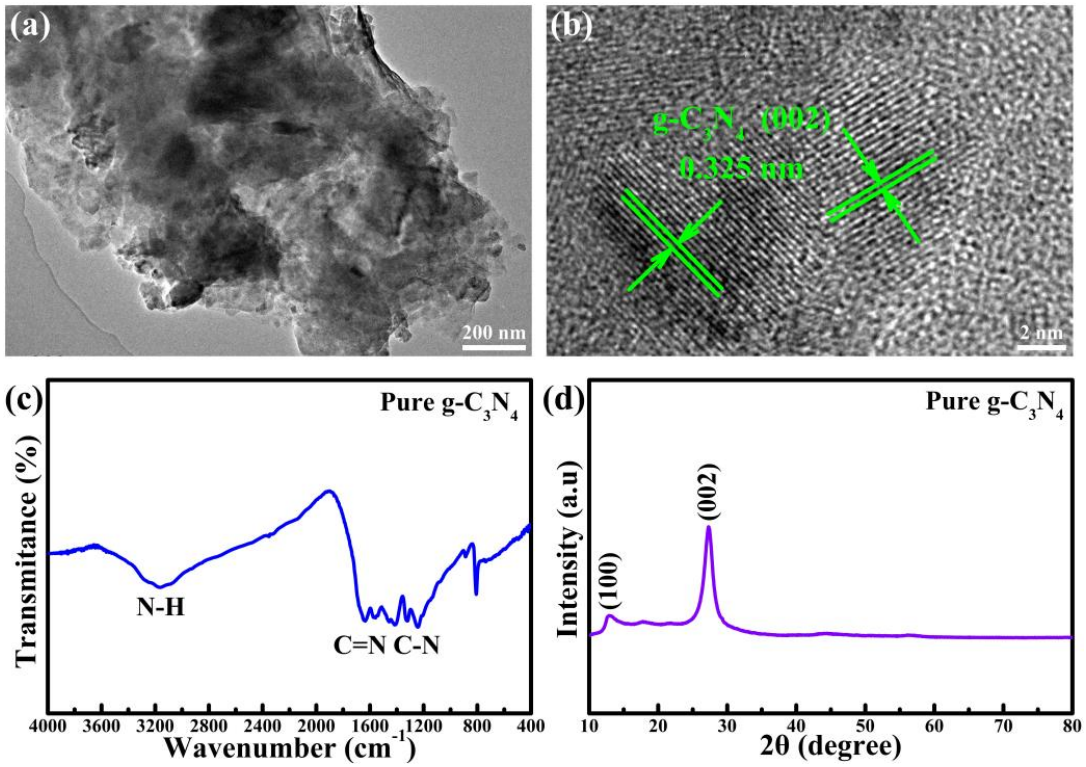

Fig. S1 (a) TEM and (b) HRTEM images for g-C_3N_4. (c) FTIR spectrum and (d) XRD pattern of g-C_3N_4.

2. XRD patterns of pure $SrTiO_3$ and Rh doped $SrTiO_3$.

For the $SrTiO_3$ (non doped Rh elements) sample, the diffraction peak positions and relative intensities of (100), (110), (111), (200), (210), (211), (220), and (310) crystal planes can be observed, which are consistent with the JCPDS No. 35-0634. After doping with Rh elements, no extra peaks were observed, implying no production of impurities in RST sample. However, a slight shift towards lower 2 theta can be observed on the (110) peak in RST than that in $SrTiO_3$. The shift can be ascribed to the be different ionic radii between Rh^{3+} (0.0665 nm), Rh^{4+} (0.060 nm) and that of Ti^{4+} (0.0605 nm). It is worth noting that, the ionic radii of Rh^{3+} and Rh^{4+} are much smaller than that of Sr^{2+} (0.118 nm), which suggests that Rh atoms replace the Ti atoms in $SrTiO_3$ crystalline structure.[2-4]

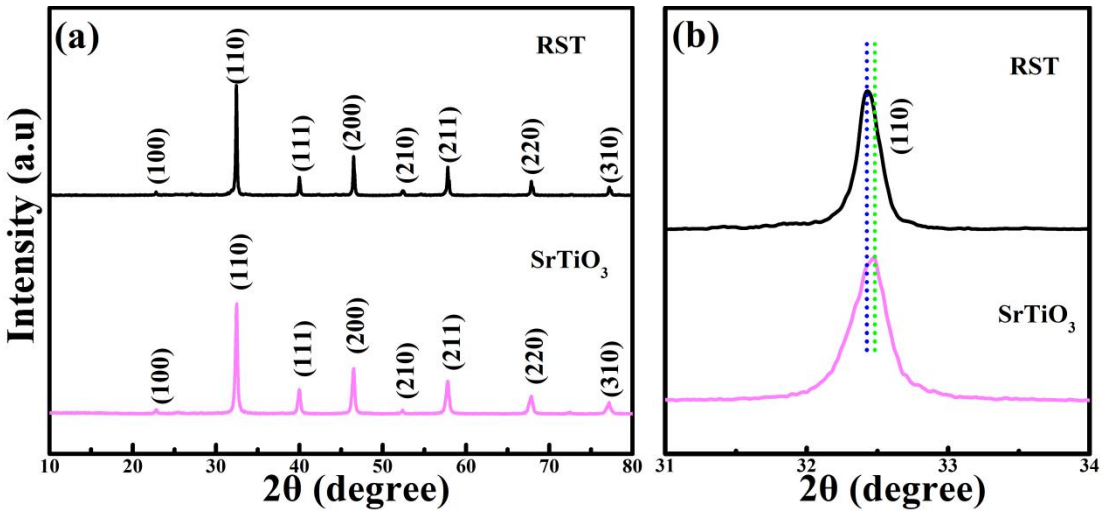

Fig. S2 (a) XRD patterns of different samples, (b) magnified area for pure $SrTiO_3$ and RST samples.

3. The PEC properties of g-C_3N_4.

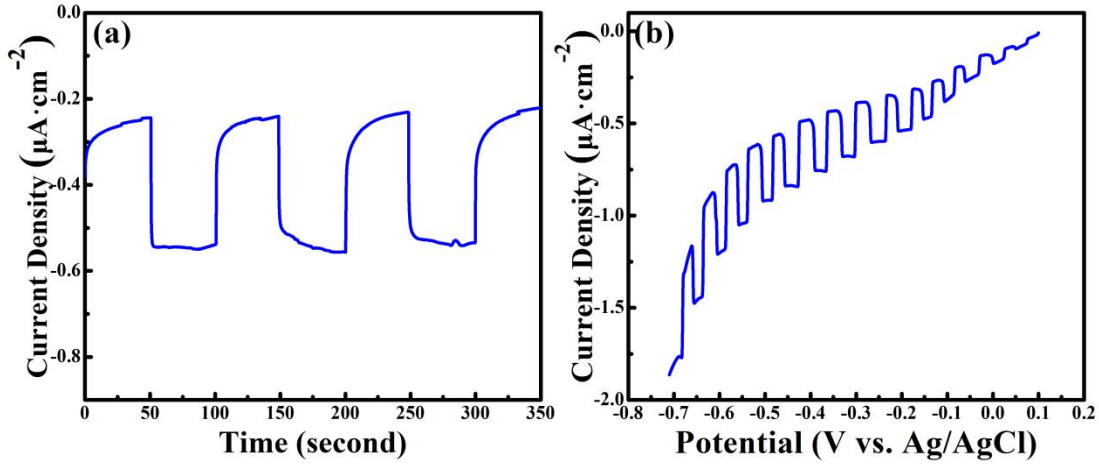

Fig. S3 PEC properties of pure g-C_3N_4 under chopped light. (a) Photocurrent versus time. (b) LSV curves.

4. Optical properties of g-C_3N_4 and $SrTiO_3$.

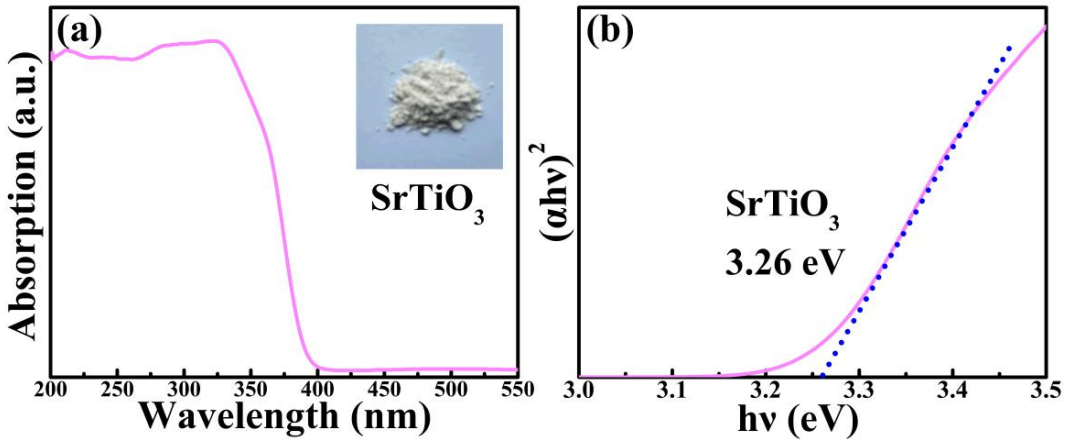

Fig. S4 (a) Absorption spectrum of $SrTiO_3$. (d) Eg value for $SrTiO_3$.

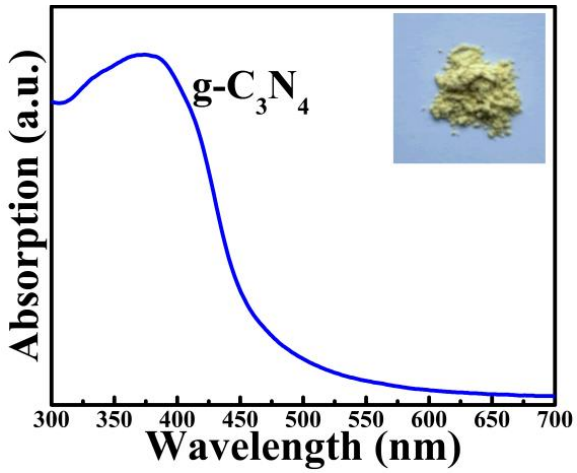

Fig. S5 Absorption spectrum of g-C_3N_4.

5. PL analysis and PL-decay of different g-C_3N_4 and RST.

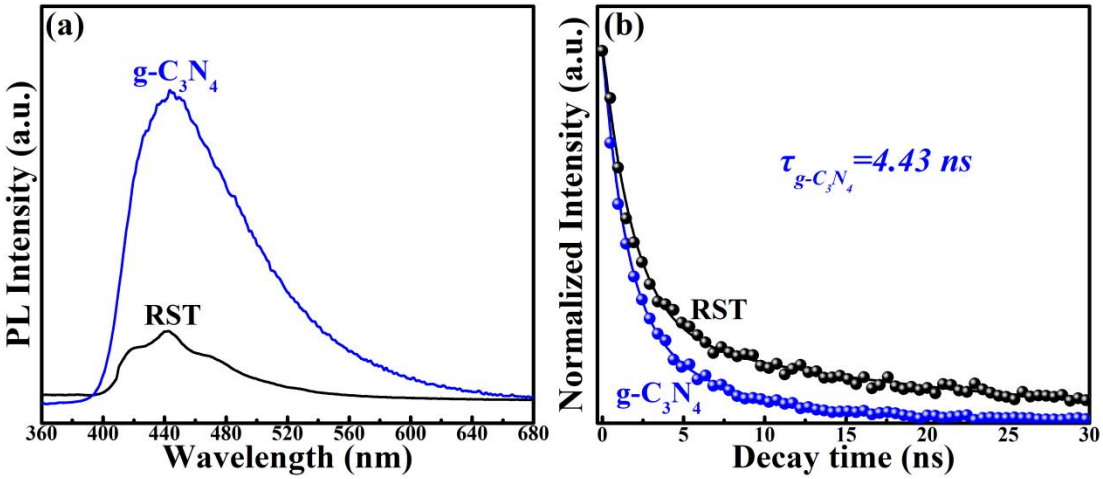

Fig. S6 (a) PL spectra of g-C_3N_4 and RST. (d) PL-decay of g-C_3N_4 and RST.

Table S1 PL-decay lifetimes of different samples.

Samples	A_1	τ_1	A_2	τ_2	τ_{total} (ns)
RST	0.23	20.8	0.71	1.88	16.67
g-C_3N_4	0.31	5.95	0.67	1.37	4.43
RSTCN7.5	0.25	24.28	0.70	2.02	20.07

6. The EIS results of different samples

Table S2 EIS results of different samples.

Samples	R_s ($\Omega \cdot cm^{-2}$)	R_{ct} ($\Omega \cdot cm^{-2}$)
RST	35.4	6769
RSTCN7.5	22.5	3699

7. Band structure of RST

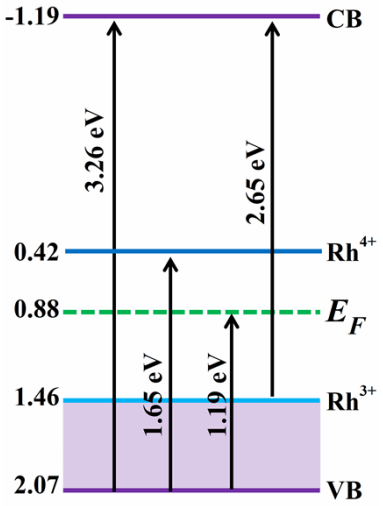

Fig. S7 Energy diagram for RST (including Rh^{4+} and Rh^{3+} levels).

References

1 L. X. Wang, Y. L. Dong, J. Y. Zhang, F. F. Tao and J. J. Xu, *J. Solid. State. Chem.*, 2022, **308**, 122878.

2 P. C. Shen, J. C. Lofaro Jr., W. R. Woerner, M. G. White, D. Su and Al. Orlov, *Chem. Eng. J.*, 2013, **223**, 200-208.

3 J. Hirayama, Ry. Abe and Y. Kamiya, *Appl. Catal. B Environ.*, 2014, **144**, 721-729.

4 M. Guo and G. J. Ma, *J. Catal.*, 2020, **391**, 241-246.